Progress In Electromagnetics Research M, Vol. 19, 39–52, 2011

THERMAL EFFECT MODELING ON PASSIVE CIRCUITS WITH MLP NEURAL NETWORK FOR EMC APPLICATION

M. Bensetti, F. Duval, and B. Ravelo*

IRSEEM, EA 4353, Graduate School of Engineering ESIGELEC, Technopole du Madrillet, Avenue Galilée, BP 10024, Saint Etienne du Rouvray Cedex 76801, France

Abstract—During the last two decades, several simulation tools have been proposed for the modeling of electronic equipments in function of the physical environmental changes. It was stated that numerous electronic components such as semiconductor devices can be affected by the mechanistic effects, humidity or simply the temperature variations. To study the last effect, based on the multilayer perceptron neural network (MLPNN), a characterization method of the passive electronic device thermal effects is introduced in this paper. The method proposed was realized toward the equivalent circuit identification of the under test device (R, L, C components) measured input impedances. To demonstrate the relevance of the method, numerical computations with MLPNN algorithms implemented into Matlab were performed. First, a capacitor modeling from 30 kHz to 1 GHz for the temperature variation from 25°C to 130°C is presented. It was found that a good agreement between the proposed model and the measurement is observed. Then, a commercial EMI low-pass filter was also characterized in RF frequencies through the S-parameter identification. Finally, further discussion on the potential applications of this work, in particular, in the electromagnetic compatibility (EMC) field is offered in the last part of this paper.

1. INTRODUCTION

Since the invention of semiconductor transistor in 1947, the development of electronic equipments increases according to the exponential law [1]. This technological progress is known with

Received 26 April 2011, Accepted 14 June 2011, Scheduled 29 June 2011
* Corresponding author: Blaise Ravelo (blaise.ravelo@yahoo.fr).

the electronic feature size shrinking and the density growth. In parallel to this spectacular development, the undesired electromagnetic compatibility (EMC) effects [2–5] and the different environmental effects [6–15] such as the humidity and the thermal influence become more and more unavoidable. Therefore, these physical aspects should be considered during the design and the fabrication of modern electric- and electronic- circuits. To deal with these issues, various modeling methods and simulator tools were proposed in the electronic engineering global market. Currently, one of most attracting ideas to many electronic engineers are those allowing to realize the multi-physic investigation such as the thermo-mechanical modeling [12, 13]. But till now, further investigations are necessary for the evaluation of the adaptability, reliability and even the durability of electric and electronic systems according to the unavoidable environmental contributions. It was reported that these unwanted effects especially, the thermal aspects can degrade severely the components for example the study at the joint interfaces of the contact resistance [9]. To ensure the reliability of the electronic equipments, these improbable environmental physical parameter variation changes need to be evaluated with an accurate modeling approach. In this way, different analytical models dedicated to the authenticity of electronic equipment behaviors, like the passive circuits versus frequency were proposed [16–20].

The present paper is focused on the investigation of the passive circuit behavior change in function of the temperature in the low- and RF- frequencies. For the achievement of more global aspect on the electronic passive circuit thermal effects, a combination of the thermal model and the reliable electronic circuit behavioral model seems to be an important concept. As argued previously, the undesired physical environment influences may affect electronic functions at different levels of embedded electronic systems. For example, in the automotive vehicle application, it was shown that the impact of the thermal variations and EMC effects can change significantly the behaviors of the functioning of different electric/electronic power system bodies like the filters, regulators, DC/DC and AC/DC converters [3–5]. In addition, as described in [6, 7], the EMC effects generate usually significant noise contributions between different blocks of telecommunication architectures. So, techniques for extracting equivalent models of certain classical components were introduced few decades ago. Mostly, the proposed models in the literature are dedicated to non-linear components such as diodes and transistors [11]. Few studies were made about the EMC modeling of passive circuits with the consideration of thermal aspects.

For this reason, this paper is presented; it is aimed to the characterization of passive device behavioral changes according to the thermal influences. To gain more insight about this method, the paper is structured in three different sections. Section 2 recalls the equivalent schematics of R, L and C basic components under consideration at the RF frequencies [17]. Then, it is completed with the main part of this paper which concerns the thermal influence modeling technique proposed. It is based on the application of the multilayer perceptron neural network (MLPNN) algorithm introduced recently in [19]. Afterward, the obtained results are validated with the polynomial approximation [20]. Thus, Section 3 presents the application of the proposed technique for the modeling of thermal influence on the commercial EMI low-pass filter. The last section draws the conclusion and the prospects.

2. STUDY OF THE THERMAL INFLUENCE ON THE PASSIVE COMPONENTS

Before starting the thermal aspect study, let us see how the considered passive components are modeled in wide frequency range. Similar to the technique introduced in [17], the proposed modeling method is based on the extraction of the under study device input impedance denoted $Z_{in}(f)$ versus frequency f. $Z_{in}(f)$ is calculated from the input reflection coefficient, $S_{11}(f)$ through the following formula:

$$Z_{in}(f) = Z_0 \frac{1 + S_{11}(f)}{1 - S_{11}(f)}, \tag{1}$$

where $Z_0 = 50\,\Omega$ is the reference impedance. Then, $Z_{in}(f)$ will be identified to the corresponding model of the tested circuit.

2.1. Recall on the Passive Component Modeling in the RF Frequencies

As stated in [16–18], the input impedance of certain realistic passive components such as resistor, inductor and capacitor can present non-neglecting scattering effects around the proposed operating frequencies. So, the consideration of such unwanted effects is crucial for the designers and manufacturers of modern electronic systems. For that, one of the simplest techniques is the application of the employed component realistic models including the parasitic elements. In this way, an accurate schematic of R, L and C component equivalent models have been established [17]. As shown in Figs. 1, these models depend on the structure and the type of the considered electronic components.

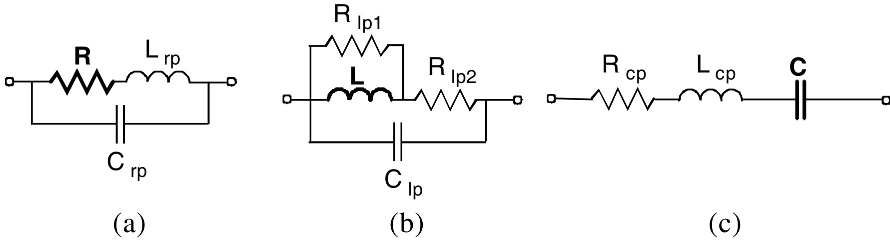

Figure 1. Equivalent circuit diagrams of real components: (a) resistor, (b) inductor and (c) capacitor with nominal value R, L and C, respectively.

Obviously, the different parasitic elements (L_{rp}, C_{rp}, R_{lp1}, R_{lp2}, C_{lp}, R_{cp}, L_{cp}) should be taken into account in the equivalent schematic due, for example, to the eventual undesired electromagnetic (EM) couplings and losses related to the Joule effect. Then, these elements are optimized by identification of the equivalent circuit impedance with the measurements.

But, it is interesting to remind that in practice, the behaviors of these parasitic elements can change strongly according to the ambient temperature variations. In the next section, one serves to the equivalent circuits represented in Fig. 1, for the exploration of the thermal influence modeling.

2.2. Thermal Influence Experimentation

During the experiment, the environmental ambient temperature was changed from 25°C to 130°C. At noted that along this subsection, the S-parameters of the tested 6.8-nF-ceramic capacitor were measured and recorded with the HP-8753D-network analyzer operating from 30 kHz to 3 GHz through the SOLT calibration after the temperature changes. Fig. 2(a) and Fig. 2(b) represent respectively the photograph of the measurement test bench available at IRSEEM laboratory and the furnace description as introduced in [21]. After temperature changes with the regulator, the vector network analyzer (VNA) was calibrated.

By using expression (1), one calculates the corresponding input impedance and optimizes the parasitic elements of the capacitor equivalent circuit shown in Fig. 1(c). Therefore, the results plotted in Fig. 3 are obtained for different values of temperature, T. In this graph, the $|Z_{in}|$ normalized values are expressed in dB and set in semi-logarithmic scale.

We emphasize that a significant right shift of the Z_{in}-resonance

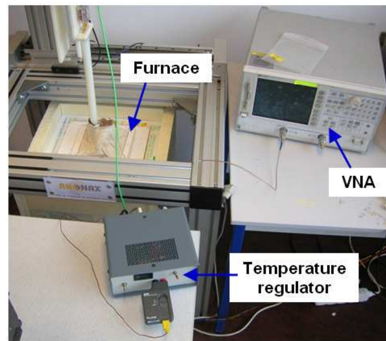

(a)

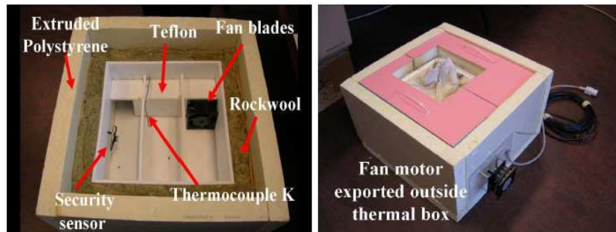

(b)

Figure 2. (a) IRSEEM thermal test bench. (b) Furnace description.

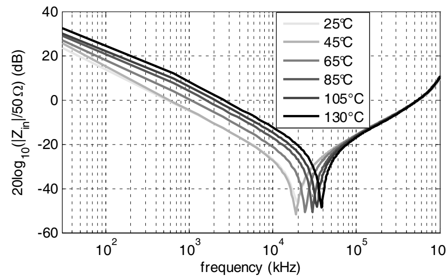

Figure 3. Illustration of the 6.8-nF-ceramic capacitor $|Z_{in}|$-variation with the temperature (from 25°C to 130°C) versus frequency (in logarithmic scale).

frequency appears when T increases. For the determination of the global model taking into account this change of Z_{in}, more general methodology using the MLPNN algorithm is deployed in the next subsection.

2.3. Modeling of the Thermal Effect with MLPNN Algorithm

The MLPNN model considered in this paper is based on the algorithm developed in [11]. In this case, we recall that the physical problem treated is non linear. For this reason, multilayer perceptron non-linear networks are chosen. The neurons are organized in several layers and they receive their input neurons from the previous layer or simply the network inputs in the case of the first layer. They transmit their output to those of the next layer. In this work, we investigated the NN structures comprised of a single hidden layer of continuous functions and nonlinear (such as the hyperbolic tangent function) and an output layer of linear functions. To determine the network architecture structures (or number of neurons in the hidden layer), several NN have been studied. For each structure, several internal initialization parameters are performed to ensure that the NN in the NN learning converges to the global minimum error criterion. The algorithm of Levenberg-Marquardt "back-propagation" was used during the learning. This algorithm reuses the steps for the output layer gradient calculation to the inner layers, thus minimizing the calculation process. For each structure, mean squared error (MSE) is considered for the validation after training. The adequate network corresponds to the structure which presents the lowest MSE on the validation dataset. The input of neural model consists of different temperatures and the output represents the impedance module as illustrated by the functioning principle diagram shown in Fig. 4. We underline that it acts as ones of the most expanded NN.

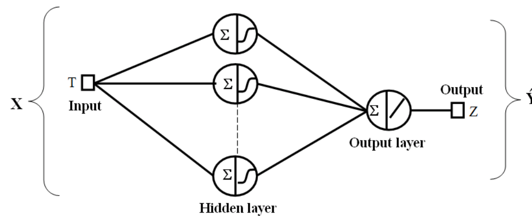

Figure 4. Illustration principle of the MLPNN algorithm.

After application of the three fundamental steps (learning, validation and test) of MLPNN training as described previously the main database of understudy 6.8-nF-capacitor model with temperature influences from 30 kHz to 1 GHz was generated. During the execution of this algorithm, it is noteworthy that the implemented routine is based on the split-sample method including 10 neurons. Consequently,

as presented in Fig. 5, a good approximation between capacitor models and measurements for $T = 60°\mathrm{C}$ and $100°\mathrm{C}$ is realized nonetheless the slight shift of the resonance frequencies which is mainly due to the MLPNN inaccuracies.

Moreover, one observes also that around the resonance, the value of $|Z_{in}|$ is very small, so, it can affect the numerical accuracy of employed calculator. But, in absolute value, this difference is seemingly neglected.

In a nutshell, this method enables to determine the database of the tested capacitor for all temperatures between 25°C and 130°C. We point out that outside the resonances where the impedance magnitude values are not significantly considerable, the relative errors are lower than 5% at $T = 100°\mathrm{C}$ and below 10% at $T = 60°\mathrm{C}$. Due to the certain resonance related to parasitic elements of components, the difference between the measurement and the model can change with the temperature as the case of results obtained here at $T = 60°\mathrm{C}$. For further evidence of this MLPNN modeling efficiency, the validation with another method based on the polynomial approximation is carried out in next subsection.

2.4. Modeling of Thermal Effect Proposed with Polynomial Approximation

From the measured input impedance of the tested capacitor in function of the temperature shown in Fig. 3, one can write polynomial expressions which govern the parameters R_{cp} (in Ω), L_{cp} (in nH) and C (in nF) versus T (in °C) by using the basic fitting tool available in

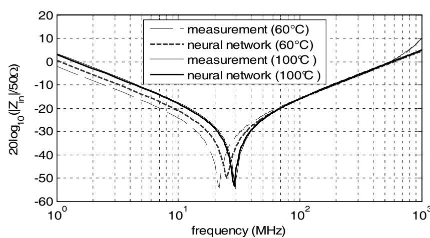

Figure 5. Comparison between the measured and optimized Z_{in} run with MLPNN versus frequency (in logarithmic scale) of a 6.8-nF-capacitor at 60°C and 100°C.

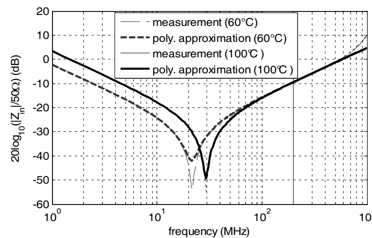

Figure 6. Comparison between the measured and polynomial approximated Z_{in}-magnitudes of tested 6.8-nF-capacitor for $T = 60°\mathrm{C}$ and $100°\mathrm{C}$.

Matlab [20]. In this case, it is interesting to note that only six degree polynomial expressions are widely enough for attaining a relative error less than 5% compared to the measurements. Therefore, one deduces the following empirical relations of parasitic- and nominal- values versus T:

$$R_{cp}(T) = 3.4 \times 10^{-11}T^6 - 1.5x \times 10^{-8}T^5 + 2.5 \times 10^{-6}T^4 - 2.1 \times 10^{-4}T^3 - 0.0089T^2 - 0.18T + 1.4, \quad (2)$$

$$L_{cp}(T) = -4.3x \times 10^{-7}T^3 - 4.5x \times 10^{-5}T^2 + 0.03T + 12, \quad (3)$$

$$C(T) = 10^{-5}T^3 - 0.0022T^2 + 0.079T + 5.1, \quad (4)$$

One recalls that the quantity T, R_{cp}, L_{cp} and C are expressed respectively in °C, Ω, nH and pF. In order to check the relevance of the above expressions, one compares the models obtained with the measurements for $T = 60°\mathrm{C}$ and 100°C. Therefore, the $|Z_{in}|$-normalized magnitude (expressed in dB) plotted in Fig. 6 are obtained. Once again, these results confirm that a good correlation with the measurements is realized in RF frequency range.

In the present section, the thermal aspect model established was applied merely to classical elementary capacitor components. For a more practical application, the next section provides a use case of the wide band modeling of a commercial electromagnetic interference (EMI) low-pass filter with the consideration of thermal effects.

3. THERMAL EFFECT MODELING OF EMI LOW-PASS FILTER BY USING MLPNN ALGORITHM

The present section shows a global modeling of an example of passive electronic device (low-pass filter) from 30 kHz to 1 GHz in function of the temperature variation. The explored MLPNN models were fitted with the measured S-parameters recorded from HP-8753D-network analyzer used previously through the SOLT calibration. In order to verify the accuracy of the circuit optimized, it will be compared with S-parameters of the under study device ideal schematic.

3.1. Description of the under Test Filter

Figure 7 presents the photograph of the under study EMI FMW 2-41-10 low-pass filter, manufactured by Timonta®. It is a four-port component generally used for the protection against the voltage interference induced in the electronic mobile equipments. As highlighted in Fig. 7, this filter is an asymmetrical circuit. After measurements of their S-parameters from 30 kHz to 1 GHz, one gets

Figure 7. Photograph of under study EMI low-pass filter.

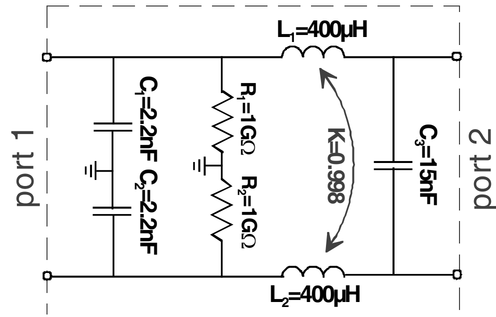

Figure 8. Ideal schematic of under study low-pass filter.

the results shown and examined in next subsection. Then, it will be exploited for generating the database of the thermal model of the under test filter through the SPICE schematic environment. It should be noted that the simulations performed in this section were run with the ADS software from Agilent®. Fig. 8 depicts the filter simulated ideal schematic proposed by the manufacturer by considering the reference source and the load impedance equal to $Z = 50\,\Omega$.

As can be seen in this diagram, the herein filter topology is constituted by classical LC-networks which are composed of series 0.4 mH-inductors L_1 and L_2 associated with parallel capacitors of some nF.

For the achievement of more realistic model of this filter, each component is replaced by its equivalent circuit introduced in Fig. 1 of Section 2. Furthermore, at noted also that, during the simulation, an empirical experimental value of $K = 0.998$ coupling coefficient was set between the two inductors of the circuit. In order to obtain correct and normalized S-parameters, a 50-Ω-source and load references have been implemented during the simulation.

3.2. Discussion on the Experimental Results

When the filter is exposed at different temperatures, as evidenced in Fig. 9, it can be found that its frequency behavior or more precisely, its S-parameters may change considerably according to its physical properties.

In addition, when the temperature is increasing here, from 25°C to 130°C, we observe also that the filter cut-off frequency is considerably shifted and its rejection is more and more degraded. These technical

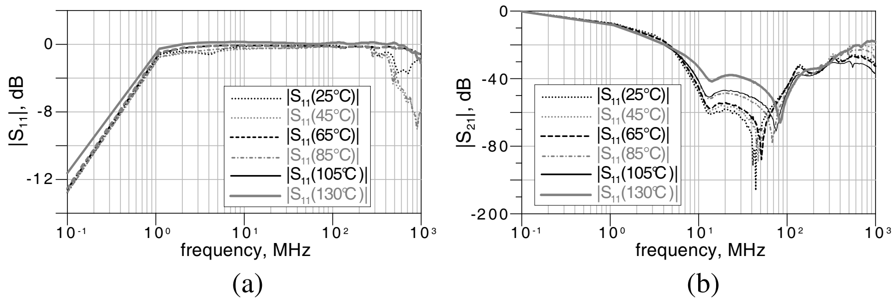

Figure 9. Measured (a) input reflection- and (b) transmission-parameters of the under study filter versus temperature.

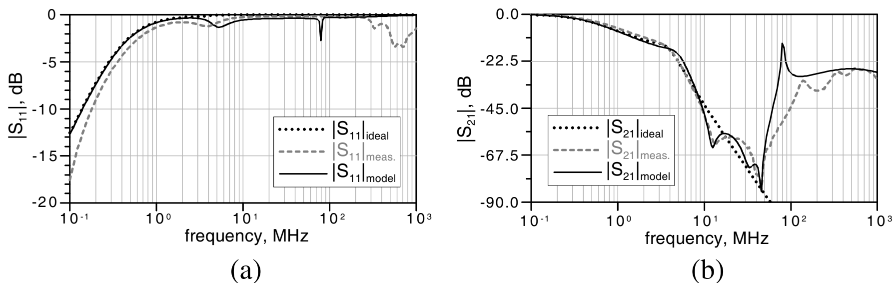

Figure 10. Comparison between the under study filter: (a) input reflection- and (b) transmission-parameters: from ideal circuit (black dashed line), measurement (grey dashed line) and proposed equivalent model (full line).

parameter sensitivities explain that the temperature variations can provoke serious problems and can damage electronic systems sensitive to the EMI perturbation.

Similar to the study leads in the previous section, from these results, the database of the S-parameter models including the temperature influences from 25°C to 130°C by using the MLPNN were elaborated. With extrapolation process, it serves as a global model of the under test filter S-parameters for any temperature in the aforementioned range value. For the verification of the functionality of the algorithm and technique proposed, comparison between ideal-, measured- and modeled-S-parameters for $T = 30°\text{C}$ was made. So, the input reflection and transmission parameters presented in Fig. 10 which are plotted in semi logarithmic scale are obtained. As depicted in Fig. 10, once again, a good agreement between ideal circuit (light gray

curve), measurement (dark gray curve) and proposed thermal model (black curve) is observed in the frequency band 30 kHz to 50 MHz. More importantly, we find also good correlations between these three curves in the filter pass-band frequency range. In addition, the measured S-parameters present a remarkable parasitic ripple beyond 60 MHz.

Such phenomenon is very difficult to forecast with the classical ideal schematic of the filter. Contrariwise, as illustrated in Fig. 10, the optimized proposed thermal model enables to characterize intriguingly this ripple effect. This confirms that the proposed global model is potentially efficient for characterizing complex electric or electronic devices/systems formed by several R, L and C components.

4. CONCLUSION AND FUTURE WORKS

A modeling technique of electric and electronic passive lumped-device characterization which takes into account the thermal effects is investigated in wide RF frequency range. Similarly to the process reported in [17], the deployed models are based on the exploitation of basic R, L, and C component equivalent circuits. These elementary models are identified through the measured input impedance of under test devices. This input impedance is deduced from the measured input reflection parameter which in turn, recorder from vector network analyzer. The efficiency of the proposed model including temperature influence, in this work considered in the range value from 25°C and 130°C, was evidenced by testing a ceramic capacitor in the frequency range from 30 kHz to 1 GHz. Then, the database of the thermal global model implemented into Matlab routine emulated thanks to the MLPNN algorithm after the learning process proposed in [19]. Therefore, it was shown that the obtained results are well-agreed to the measurements for whatever the ambient temperature values between 25°C and 130°C. For more concrete practical verification of the proposed model utility, a more sophisticated electronic device which acts as an EMI commercial FMW 2-41-10 low-pass filter was experimented and characterized. Therefore, tests from 50 kHz to hundreds of MHz were performed by changing surrounding filter temperature in same range value as previously. By using the elementary R, L and C- thermal models, reflection and transmission parameters well-agreed with measurements whatever considered the environmental temperatures, different to those considered during the learning process of MLPNN are realized.

To sum up, a method of electronic device global model was devoted by employing a MLPNN routine here implemented in Matlab

environment. Then, with the extrapolation process generated in NN databases, a possibility of electronic passive device characterization from kHz up to GHz in function of the temperature is demonstrated. So, in terms of application, this model can serve for predicting high frequency parasitic effects which can create the EMC degradation during the design of the electronic circuits especially for the power systems.

As prospect of this work, the transposition of the under consideration approach applied to more sophisticated circuits as active devices or mechatronic systems by including simultaneous effects of other multi-physic environmental parameters (humidity, mechanical chocks...) is currently in progress. So, we envisage optimistically that the present technique should be an interesting line of engineering research for the treatment of conducting EMC problems in numerous embedded electronic systems.

ACKNOWLEDGMENT

Acknowledgement is made to mov'eo (Upper-Normandy region cluster in FRANCE) and Asystematic (Paris region cluster) for the support of this research work through O2M (*Outils de Modélisation et de conception Mécatronique*) program.

REFERENCES

1. Moore, G. E., "Cramming more components into integrated circuits," *Electronics*, Vol. 38, No. 8, 114–117, 1965.
2. Renault, "Resistance to electrical disturbances and electromagnetic compatibility instructions concerning electrical, electronic and pyrotechnic equipment," Product Specification 36-00-808/–G, Rev. D, Oct. 2000.
3. Williams, B. W., "Principles and elements of power electronics, devices, drivers, applications, and passive components," Free eBook:share_ebook, 986, 2006, ISBN 978-0-9553384-0-3.
4. Neugebauer, T. C. and D. J. Perreault, "Filters with inductance cancellation using printed circuit board transformers," *Proc. PESC'03, IEEE 34th Annual Conf.*, Vol. 1, 272–282, 2003.
5. Wang, S., F. C. Lee, D. Y. Chen, and W. G. Odendaal, "Effects of parasitic parameters on EMI filter performance," *IEEE Trans. Power Electronics*, Vol. 19, No. 3, 869–877, May 2004.
6. Mawby, A., P. M. Igic, and M. S. Towers, "New physics-based compact electro-thermal model of power diode dedicated to circuit

simulation," *Proc. IEEE ISCAS 2001*, Vol. 2, 401–404, Sydney, Australia, May 2001.

7. Vuolevi, J. and T. Rahkonen, "Extracting a polynomial ac FET model with thermal couplings from S-parameter measurements," *Proc. IEEE ISCAS 2001*, Vol. 2, 461–464, Sydney, Australia, May 2001.
8. Renken, F., "High temperature electronics for future hybrid drive systems," *13th European Conf. on Power Electronics and Applications, Proc. EPE-PEMC 2009, 14th Int. Power Electronics and Motion Control Conf.*, Barcelona, Spain, Sep. 8–10, 2009.
9. Song, S. and K. P. Morgan, "Thermal and electrical resistances of bolted joints between plates of unequal thickness," *Semiconductor Thermal Measurement and Management Symp., 1993, SEMI-HERM IX., Ninth Annual IEEE*, 28–34, Austin, TX, USA, Feb. 1993.
10. Wagner, D., "Modeling thermal effects in RF LDMOS transistors," MOTOROLA Semiconductor Application Note, 1–7, AN1941, 2002.
11. Suter, P., R. Bauknecht, T. Graf, H. Duran, and I. Venter, "Thermo-mechanical finite-element modeling of a chip-on-foil bonding process," *Proc. of the 6th Inter. Conf. on Thermal, Mechanical and Multi-physics Simulation and Experiments in Micro-electronics and Micro-systems, EuroSimE 2005*, 25–30, Apr. 18–20, 2005.
12. Deplanque, S., W. Nuchter, M. Spraul, B. Wunderie, R. Dudek, and B. Michel, "Relevance of primary creep in thermo-mechanical cycling for life-time prediction in Sn-based solders," *Proc. of the 6th Int. Conf. on Thermal, Mechanical and Multi-physics Simulation and Experiments in Micro-electronics and Micro-systems, EuroSimE 2005*, 71–78, Apr. 18–20, 2005.
13. Sagkol, H., S. Sinaga, J. N. Burghartz, B. Rejaei, and A. Akhnoukh, "Thermal effects in suspended RF spiral inductors," *IEEE Electron. Device Letters*, Vol. 26, No. 8, 541–543, 2005.
14. London, S., D. Fricano, A. Dasgupta, T. Reinikaininen, G. Freitas, and C. Pagliosa, "Probabilistic effects in thermal cycling failures of high-I/O BGA assemblies," *Proc. of the 10th Int. Conf. on Thermal, Mechanical and Multi-physics Simulation and Experiments in Micro-electronics and Micro-systems, EuroSimE 2009*, 1–7, Apr. 26–29, 2009.
15. Jian-Ping, L., Y. Ping, Z. Jian, C. Quayle, C. Jing, L. Xu, and A. Salo, "Thermal analysis based on the environmental tests of STN display," *Proc. of the 10th Int. Conf. on Thermal,*

Mechanical and Multi-physics Simulation and Experiments in Micro-electronics and Micro-systems, EuroSimE 2009, 1–6, Apr. 26–29, 2009.

16. Bowick, C., "RF circuit design," *Elsevier Science*, Burlington, 1982.
17. Pena, A. E., M. Bensetti, F. Duval, and B. Ravelo, "Modeling of passive components from the measured S-parameters and application for low-pass filter characterization," *Proc. of EPE-PEMC 2010, 14th Int. Power Electronics and Motion Control Conf.*, Ohrid, Republic of Macedonia, Sep. 6–8, 2010.
18. Naishadham, K., "Experimental equivalent circuit modeling of SMD inductors for printed circuit applications," *IEEE Trans. EMC*, Vol. 43, No. 4, 557–565, 2001.
19. Bensetti, M., Y. Le Bihan, and C. Marchand, "Non-destructive evaluation of layered planar media using MLP and RBF neural networks," *The 8th International Workshop on Electromagnetic Nondestructive Evaluation*, Saarbrucken, Allemagne, 2002.
20. http://www.mathworks.fr/.
21. Malki, M. A., D. Baudry, and M. Ramdani, "New tool for characterizations of electronic components radiated emissions under thermal constraints," *EMC Compo 09*, Toulouse, France, Nov. 2009.